



**HAL**  
open science

## One-year ageing FTIR monitoring of PE/EVOH/PE film after gamma or electron beam irradiation

Nina Girard-Perier, Samuel Dorey, Fanny Gaston, Fabien Girard, Sylvain R.A. Marque, Nathalie Dupuy

### ► To cite this version:

Nina Girard-Perier, Samuel Dorey, Fanny Gaston, Fabien Girard, Sylvain R.A. Marque, et al.. One-year ageing FTIR monitoring of PE/EVOH/PE film after gamma or electron beam irradiation. *Polymer Degradation and Stability*, 2022, 195, pp.109790. 10.1016/j.polymdegradstab.2021.109790 . hal-03739287

**HAL Id: hal-03739287**

**<https://hal.science/hal-03739287>**

Submitted on 20 Feb 2023

**HAL** is a multi-disciplinary open access archive for the deposit and dissemination of scientific research documents, whether they are published or not. The documents may come from teaching and research institutions in France or abroad, or from public or private research centers.

L'archive ouverte pluridisciplinaire **HAL**, est destinée au dépôt et à la diffusion de documents scientifiques de niveau recherche, publiés ou non, émanant des établissements d'enseignement et de recherche français ou étrangers, des laboratoires publics ou privés.

# One-year ageing FTIR monitoring of PE/EVOH/PE film after gamma or electron beam irradiation

Nina Girard-Perier<sup>a</sup>, Samuel Dorey<sup>a,\*</sup>, Fanny Gaston<sup>a</sup>, Fabien Girard<sup>b</sup>,  
Sylvain R.A. Marque<sup>c,\*</sup>, Nathalie Dupuy<sup>b,\*</sup>

<sup>a</sup> Sartorius Stedim FMT S.A.S, Z.I. Les Paluds, Avenue de Jouques CS91051, Aubagne CEDEX 13781, France

<sup>b</sup> Aix Marseille Univ, Avignon Université, CNRS, IRD, IMBE, Marseille, France

<sup>c</sup> Aix Marseille Univ, CNRS, ICR, Case 551, Marseille 13397, France

## ARTICLE INFO

### Article history:

Received 25 June 2021

Revised 23 November 2021

Accepted 25 November 2021

Available online 27 November 2021

### Keywords:

FTIR

Gamma irradiation

Electron beam irradiation

Multilayer film

Principal component analysis

Polyethylene

## ABSTRACT

The effects of gamma and electron beam irradiation on PE/EVOH/PE film used in biopharmaceutical and biotechnological applications were screened using Fourier Transform Infrared (FTIR) spectroscopy combined with chemometric treatment. The modifications induced by different irradiation doses (25 and 50 kGy) and different post irradiation ageing periods (1, 6 and 24 months) were studied. Results show that shortly after irradiation gamma irradiated and non-sterilized samples exhibit a different behavior than electron beam irradiated samples, whereas 6 months after irradiation gamma irradiated samples are similar to electron beam irradiated samples from a polymer arrangement point of view.

## 1. Introduction

Sterilization is used as a required and standardized process in a wide variety of industrial areas such as the medical device industry, the manufacturing of single use multilayer plastic film systems for biopharmaceutics, and parenteral drugs. Using radiation in sterilization has an invaluable advantage due to its significantly low residual toxicity. Gamma irradiation has been used for many years in the sterilization process, and new alternative modalities are emerging such as electron beam and X-ray irradiation [1–5]. In this article we focused first on the irradiation by electron beam. Electron beam sterilization is increasingly applied to materials as well as to pharmaceutical or food products. Since the commercialization of the electron beam more than 50 years ago, a lot of research has been done on its effects on pharmaceutical products [6–10]. In the medical [11] and pharmaceutical fields, polymers are present in many medical devices such as syringes, gloves, or single-use plastic bags. They are also used for biomaterials – biological or synthetic materials that can be introduced into body tissues as part of an implanted medical device. For food packaging, where irradiation is used for its combined, bactericidal and

fungicidal actions, the degradation of irradiated polymers is studied [12,13].

Polymers undergo changes upon exposure to radiation. These changes are influenced by some factors, such as the chemical composition of the polymers, the presence of additives or the presence of oxygen in the environment during irradiation. The phenomena occurring in the irradiated polymers involve the formation of radicals [14], changes [15–21] in polymer molecular weights due to crosslinking and/or chain scission, discolorations, and formation of oxidized molecules.

In this article, the effects of electron beam irradiation on polymers are discussed in comparison to those of gamma irradiation. In sharp contrast to most of the articles in literature, our approach aims to be as close as possible to the industrial conditions of irradiations as well as for the materials used. As our results must have industrial impacts, we intentionally performed experiments in industrial conditions as much as possible. Thus, the impact of two irradiation sources – e-beam and <sup>60</sup>Co- $\gamma$  – is investigated in industrial conditions. Gamma irradiation exposes the product to photons formed with the self-disintegration of <sup>60</sup>Co, at a dose rate of a few kGy/h. Electron beam irradiation exposes the material to high energy electrons, generated when electrons are accelerated by an electromagnetic field in an accelerator, at a dose rate of a few thousand kGy/h. For both irradiation modalities, a sterility assurance level (SAL) of 10<sup>-6</sup> can be achieved [13]. The advantages

\* Corresponding authors.

E-mail addresses: samuel.dorey@sartorius.com (S. Dorey), sylvain.marque@univ-amu.fr (S.R.A. Marque), nathalie.dupuy@univ-amu.fr (N. Dupuy).

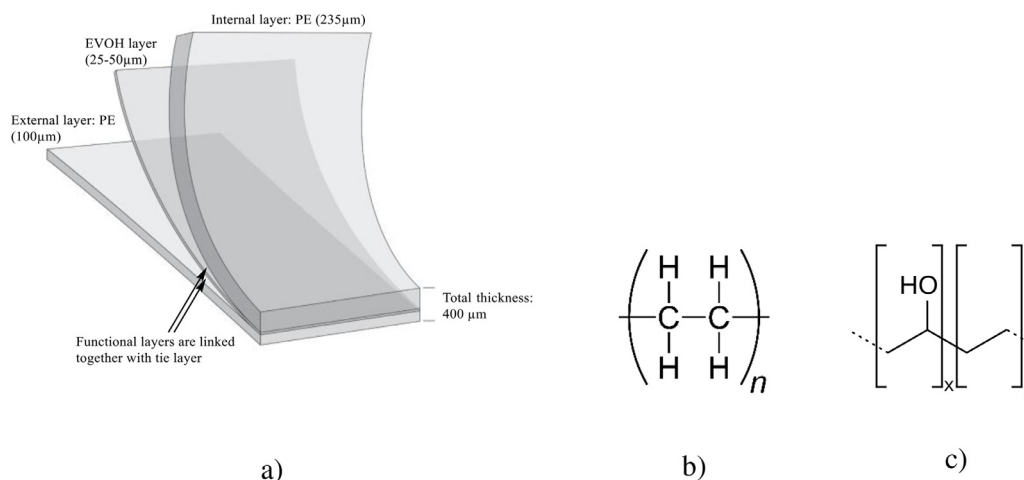


**Fig. 1.** Structure of PE/EVOH/PE (a), structure of PE (b) and EVOH (c).

**Table 1**  
Advantages and drawbacks of gamma and electron beam sterilization [24].

	Advantages	Drawbacks
Gamma sterilization	High penetration: gaseous, liquid, solid materials, homogeneous and heterogeneous systems	Dose rate lower than for electron beam Radioactive source → environmental and sustainability issues
E- beam sterilization	Need of very short exposition time Very safe method → An on-off technology that operates with electrical energy High dose rate	Low penetration High DUR (Dose Uniformity Ratio) Electricity consumption

and drawbacks [22,23] of the two modalities are summarized in Table 1.

The aim of this work was to study the effects of gamma radiation and electron beam on the surface of the multilayer polyethylene (PE)/ethylene vinyl alcohol (EVOH)/PE (also called PE/EVOH/PE) films at different doses (25, 50 and 100 kGy) using mid infrared spectroscopy, with the same non-irradiated film being our reference. FTIR spectra were recorded and sampled at three different ageing: immediately after irradiation, 6 months, and 24 months after irradiation to check changes generated by the gamma and electron beam irradiation in the multilayer PE/EVOH/PE film. The Principal Component Analysis (PCA) method was used to magnify the effects of the weak variations of the FTIR spectra recorded from the gamma and electron beam irradiated multilayer films.

## 2. Materials and methods

### 2.1. Film sample

The PE/EVOH/PE film is composed of three layers, and its total thickness is 400 μm. The structure of the film is depicted in Fig. 1. Analysis were performed on the internal and external layers. As results are similar for internal and external layers, only the internal layer results are shown and discussed in this article. To take into account the lot effect, two different lots were studied.

### 2.2. Storage conditions

Before irradiation each sample bag was placed in over pouches and a partial vacuum (not controlled) has been performed according to internal industrial procedures. However, materials were not O<sub>2</sub>-degassed, and therefore contain some level of O<sub>2</sub>. The over-pouches were placed in the cardboard and then irradiated. After irradiation and before analysis, cardboards were stored in dark, in an air-conditioned room at 20 ± 2 °C.

**Table 2**  
Gamma irradiation time detail.

Dose (kGy)	29	59	106	260
Time of exposure (hours)	~12	~34	~50	~105
Steps	3	4	5	7

### 2.3. Gamma irradiation

The PE/EVOH/PE films were wrapped in multilayer Polyethylene/Polyamide (PA)/polyethylene (also called PE/PA/PE) over pouches. These over pouches were placed in the cardboard and irradiated at the irradiator bunker temperature (40 ± 10 °C) with a <sup>60</sup>Co gamma source at Ionisos, Dagneux, France. (A picture of the plant is shown Fig. 1 in SI file). The dose rate provided was 1–2 kGy/h. Successive gamma irradiation cycles were performed to deliver the targeted dose. Between the irradiation cycles, storage times were necessary and lasting typically from two days to weeks, to allow the appropriate dosimetry to be achieved. The details of time of exposure is shown in Table 2. The doses averages were 29 kGy (±3), 59 kGy (±3) and 106 kGy (±5).

Conventional irradiation chemical processes are expected in each layer: radiation chemistry occurs in all layers as gamma radiations are largely able to reach all points of such thin materials.

### 2.4. Electron beam irradiation

Bags made from PE/EVOH/PE film were individually wrapped in multilayer PE/PA/PE packaging and placed side by side in an 8 cm thin cardboard box so as to have the same and only thickness of plastic material. (A picture of the plant is shown Fig. 2 in SI file). Samples were irradiated in a 10 MeV Rhodotron (Ionisos, Chaumesnil, France) with a power source at 28 kW, the dose rate being 18 MGy/h. Alanine dosimeters were used on the cardboard to assess the radiation delivered (±5%) to the single use bag sam-

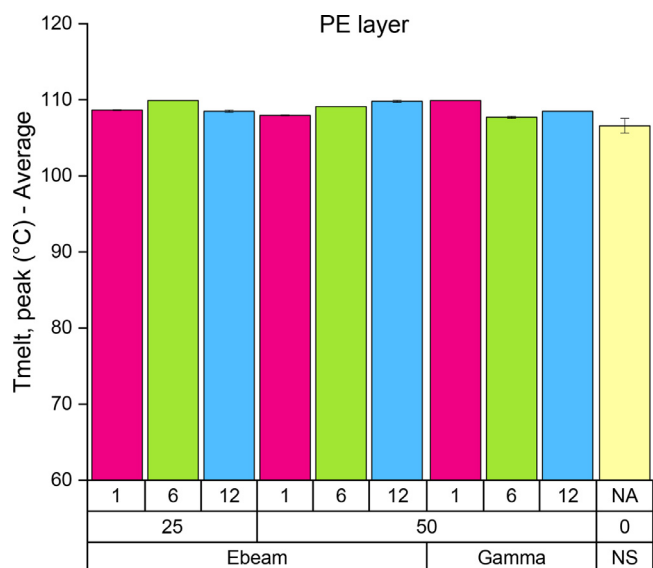


**Fig. 2.** Melting point for the PE material used in the PE/EVOH/PE multilayer film according to the ageing (months), the dose (kGy) and the irradiation modality.

ples. The average surface dose delivered was 25 and 51 kGy for double sided irradiation.

### 2.5. Fourier transform infrared spectroscopy (FTIR)

The internal face of the PE/EVOH/PE film samples ( $12 \times 10$  cm) were analyzed onto the Bruker “Golden Gate” attenuated total reflectance accessory provided with a diamond crystal. The spectra for each sample were recorded from 4000 to  $700\text{ cm}^{-1}$ , with  $4\text{ cm}^{-1}$  resolution and 64 scans, on a Thermo Nicolet Avatar spectrometer equipped with an MCT/A detector, an Ever Glo source, and a KBr/Ge beam splitter. The spectrometer was placed in an air-conditioned room at  $22\text{ }^\circ\text{C}$ . Five spectra were recorded at different locations on the film for each sample to average the potential film inhomogeneity and measurement variability. A background scan in air (under the same resolution and scanning conditions as those used for the samples) was carried out before the five sets of acquisition. The ATR plate was cleaned in situ by scrubbing with an ethanol solution to remove any residual traces of the previous sample. Cleanliness was checked by recording a background signal. The penetration depth in the sample was of a few micrometers, depending on the IR wavelength.

### 2.6. Differential scanning calorimetry (DSC)

The melting temperature of each polymer which composed the multilayer film was determined using differential scanning calorimetry. Samples (20 mg) of PE/EVOH/PE multilayer film were introduced in the DSC device. Measurements were performed with a calorimeter Sensys Evo Setaram. The heating range was  $23\text{--}250\text{ }^\circ\text{C}$ , and the heating rate was  $10\text{ }^\circ\text{C}/\text{min}$ . During the DSC experiments, air and  $\text{N}_2$  were used as gaseous environments ( $\text{N}_2$  flow:  $16\text{ mL}/\text{min}$ ). Four sample batches were investigated. Results are displayed as the average of these four batches. The second heating was considered to disregard the thermal history of the material. The statistical errors are calculated on the four batches.

### 2.7. Principal component analysis (PCA)

PCA is a multivariable technique used to reduce a large set of variables into a smaller set of variables named “principal components” [25]. The principal components represent the largest vari-

ance in the original variables. The variations in intensity and shift of the FTIR peaks were investigated. Spectra were adjusted prior to the PCA investigation using the baseline and Standard Normal Variate (SNV) correction. The derivative was performed using the Savitzky Golay algorithm. All computations were performed using the Unscrambler X 10.5 software. More details regarding PCA are provided in SI.

### 2.8. Storage conditions

The samples were stored in the boxes in dark after irradiation. After gamma and electron beam sterilization, recording was performed over time at three different times: 1, 6 and 24 months (A1, A6, A6–40  $^\circ\text{C}$ ). A1 and A6 samples were analyzed after 30 and 180 days, respectively, at room temperature whereas A6–40  $^\circ\text{C}$  samples were analyzed after 235 days at  $40\text{ }^\circ\text{C}$  (to simulate 24 months at room temperature). This corresponding time was calculated based upon the ASTM F1980 regulation [26] using  $Q10 = 2$ .

## 3. Results and discussion

After gamma and electron beam irradiation, any significant changes in the structure of each layer of the PE/EVOH/PE multilayer film should lead to significant changes in DSC. Interestingly, melting temperature given by DSC of PE/EVOH/PE film (Fig. 2) do not show significant dependence both on the modality of irradiation, on the procedure of irradiation, on doses, and ageing meaning that macroscopic or material properties are not significantly altered. However, it does not prevent to observe significant changes by spectroscopy leading to change in chemical properties, as discussed hereafter.

After gamma and electron beam irradiation, the PE/EVOH/PE multilayer film samples exhibit similar MIR (Mid-Infrared) spectra (Fig. 3) displaying the characteristic bands of aliphatic hydrocarbons:  $\nu_{\text{as}}\text{CH}_2$ :  $2916\text{ cm}^{-1}$ ,  $\nu_{\text{s}}\text{CH}_2$ :  $2848\text{ cm}^{-1}$ ,  $\delta_{\text{as}}\text{C-H}$  in  $\text{CH}_2$  groups:  $1467\text{ cm}^{-1}$ ,  $\delta\text{CH}_2$  in  $-(\text{CH}_2)_n$  ( $n > 3$ ):  $717\text{ cm}^{-1}$ . The ATR-FTIR signal (see Table 1 in SI for the assignments of the IR bands

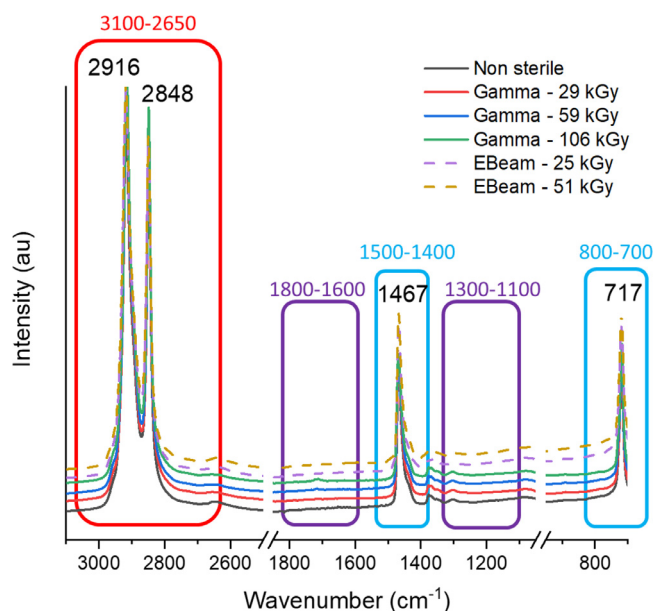
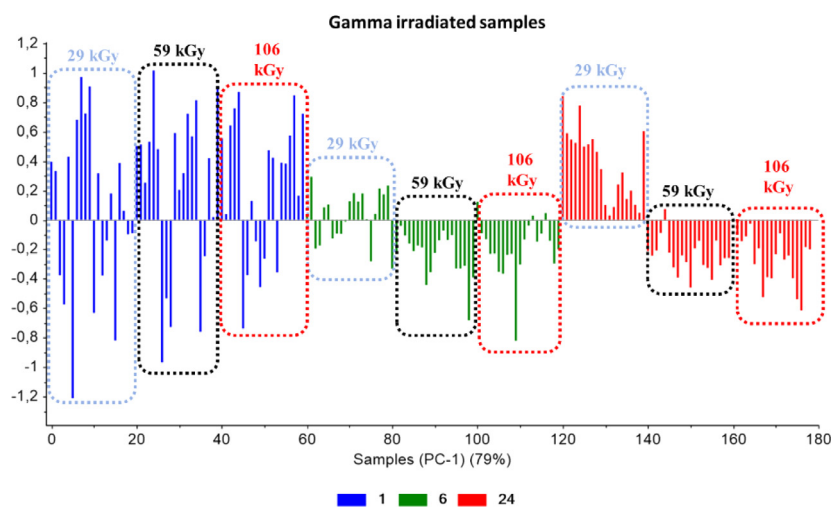
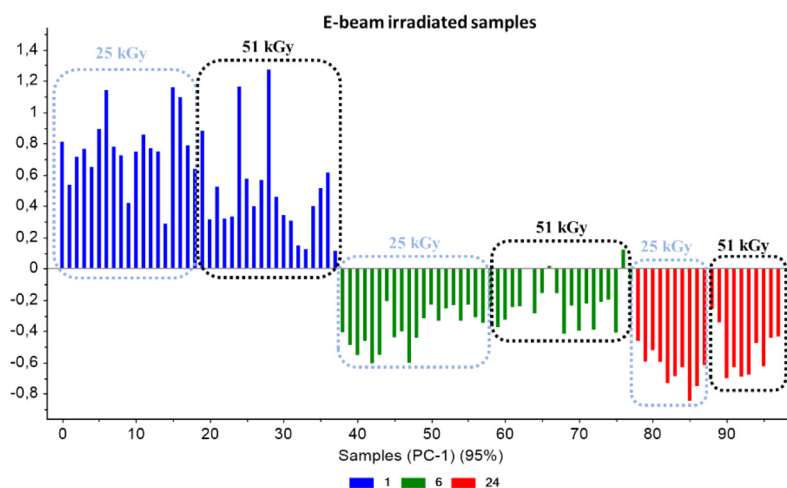


**Fig. 3.** ATR FTIR spectra for all gamma and electron beam doses on PE/EVOH/PE film: red boxes for  $\text{CH}_2$  stretching [ $3100\text{--}2650\text{ cm}^{-1}$ ], blue boxes for crystallinity peaks [ $1500\text{--}1400$ ;  $800\text{--}700\text{ cm}^{-1}$ ] and purple boxes for oxidation peaks [ $1800\text{--}1600$ ;  $1300\text{--}1100\text{ cm}^{-1}$ ]. From bottom to top IR signal for 0, 29, 59, 106 kGy doses for gamma irradiation and 25 and 51 kGy doses for electron beam irradiation (dotted lines).



a)



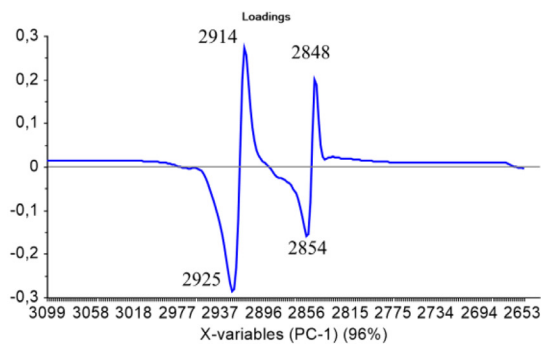
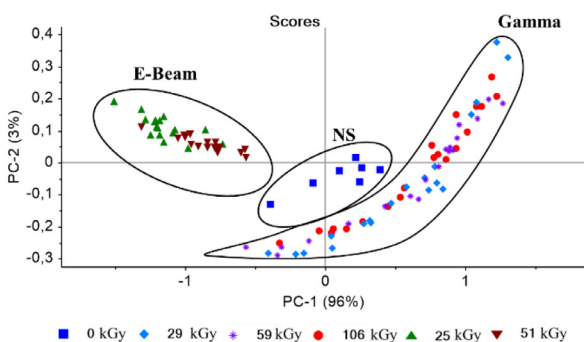
b)

**Fig. 4.** Colors according to ageing (blue for 1 month, green for 6 months, red for 24 months). PCA scores for all gamma irradiated sample spectra (29, 59 and 106 kGy) (a) and electron beam irradiated sample spectra (25 and 51 kGy) (b) after baseline and SNV correction for the zone 3100–2650  $\text{cm}^{-1}$ .

according to literature [27]) is divided in three zones. The first zone, 3100–2650  $\text{cm}^{-1}$  (red box in Fig. 3) corresponding to the stretching of  $\text{CH}_2$  groups is separated from the other PCA evaluations by its high peak intensity. The second zone, 1500–1400 & 800–700  $\text{cm}^{-1}$  (blue boxes in Fig. 3) highlights the potential modifications in crystallinity. The third zone, 1800–1600 & 1300–1100  $\text{cm}^{-1}$  (purple boxes in Fig. 3) related to the generation of oxidation products. The spectra recorded for all samples (0 kGy - non-sterilized material, gamma irradiation doses 29, 59 and 106 kGy and electron beam irradiation 25 and 51 kGy) are displayed in Fig. 3. Each zone is discussed separately as it corresponds to different chemical events affecting in various fashions the polymer structures. Moreover, part of these changes are also time dependent and discussed along this aspect.

For the spectral zone 3100–2650  $\text{cm}^{-1}$  after one month ageing A1, Fig. 4 shows the impact of ageing for gamma irradiated

samples (Fig. 4a) and electron beam irradiated samples (Fig. 4b) following the first component analysis (79 and 95% for gamma and electron beam irradiated samples, respectively). In Fig. 4a, one month after irradiation (blue), 29, 59 and 106 kGy gamma irradiated samples are distributed on each side of the axis. This means that there is no impact of the gamma irradiation dose for the samples analyzed one month post irradiation. The same comments hold for 29 kGy gamma irradiated samples analyzed six months after irradiation. However, the negative distribution for 59 and 106 kGy gamma irradiated samples analyzed six months after irradiation denotes a significant impact of irradiation. For 6 months-40 °C after irradiation, the impact of irradiation is also observed at 29 kGy (positive distribution) as well as at 59 and 106 kGy (negative distribution). In Fig. 4b, the one month aged electron beam irradiated samples (blue) are in the positive part of the graph whereas the 6 and 6–40 °C month aged electron beam irradiated



a)

b)

**Fig. 5.** One-month ageing. a) PCA for all spectra at all absorbed doses for zone 3100–2650  $\text{cm}^{-1}$  after baseline and SNV correction. b) Loading plot of PC1.

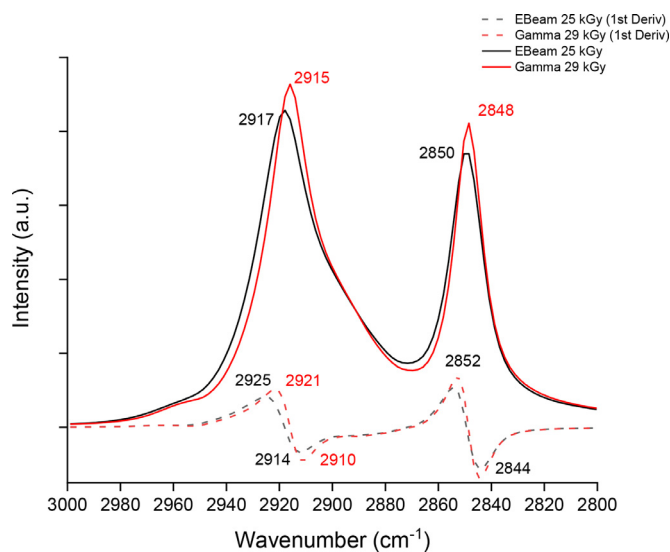
samples (green and red, respectively) are in the negative part of the graph. This means that electron beam irradiated samples seem to be modified 1 month post irradiation and never return to their initial state. There is an impact of the ageing which is not dose dependent. The same evolution for gamma and electron beam irradiated samples for the other spectral zones is observed (not shown). For the sake of clarity, the discussion of each spectral zone is carried out for each ageing period (i.e., A1, A6 and A6–40 °C months).

The zone 3100–2650  $\text{cm}^{-1}$  is ascribed to the stretching of the  $\text{CH}_2$  groups. For one month ageing, a group for electron beam irradiated, gamma irradiated, and non-sterilized samples are observed on the plot PC1 vs PC2 (Fig. 5a) accounting for 99% of the total variance. A slight difference is observed between non-sterilized and gamma irradiated samples.

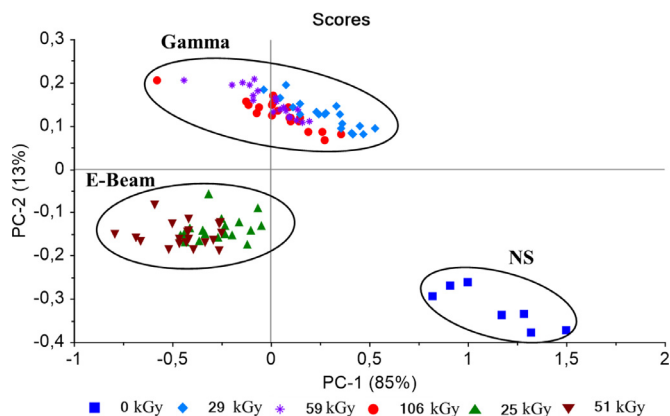
Gamma irradiation and non-sterilization values are mostly positive in PC1 (Fig. 5a), and their corresponding typical variables on the loading plot (Fig. 5b) are 2914 and 2848  $\text{cm}^{-1}$ . Conversely, 2925 and 2854  $\text{cm}^{-1}$  correspond to electron beam irradiated samples values. The first derivative form observed on the loading plot (Fig. 5b) originates from the peak shift observed in the spectra. A slight dose effect is observed for electron beam irradiated samples whereas no dose effect is observed for gamma irradiated samples.

Fig. 6 shows an overlay of signals observed after electron beam and gamma irradiation. The repeatability of gamma and electron beam spectra is shown in Fig. 3 in SI. Electron beam irradiated sample spectra are slightly less strong than gamma irradiated sample spectra, denoting a lower number of  $\text{CH}_2$  groups after sterilization by electron beam irradiation, which might be due to a higher number of crosslinking events. The environment of the  $\text{CH}_2$  groups is also slightly modified, as denoted by a signal peak shift observed after electron beam irradiation. The electron beam irradiated samples show a higher number of crosslinking events probably due to the modality of radiation.

For six month ageing, in the zone 3100–2650  $\text{cm}^{-1}$ , three groups are observed on the plot PC1 vs PC2 (Fig. 7a) accounting for 98% of the total variance: one group for of electron beam irradiated samples, one group for gamma irradiated samples, and one group for non-sterilized samples. The loading plot is identical to the one observed for 1-month ageing (Fig. 5b) and is shown in Fig. 4-SI. Over time, the behavior of gamma irradiated samples differs more and more from that of non-sterilized samples and resembles more and more that of the electron beam samples. This means that gamma and electron beam irradiated samples undergo a post-irradiation evolution, as already shown in Fig. 4. The peak intensity in the 3100–2650  $\text{cm}^{-1}$  range for the gamma irradiated samples decreased and became comparable to that for the electron beam irradiated samples (Fig. 8). Gamma irradiated samples



**Fig. 6.** Overlay of derived (after SNV treatment) and pristine sample spectra, for electron beam and gamma irradiated samples at ~25 kGy - 1 month after irradiation - spectral zone [3100–2650  $\text{cm}^{-1}$ ].



**Fig. 7.** Six-month ageing. a) PCA for all spectra at all absorbed doses for zone (3100–2650  $\text{cm}^{-1}$ ) after baseline and SNV correction.

seem to undergo crosslinking reactions over time as electron beam irradiated samples do from 1 month after irradiation. It is important to keep in mind that the spectroscopic differences observed between gamma and electron beam irradiated samples are approx-

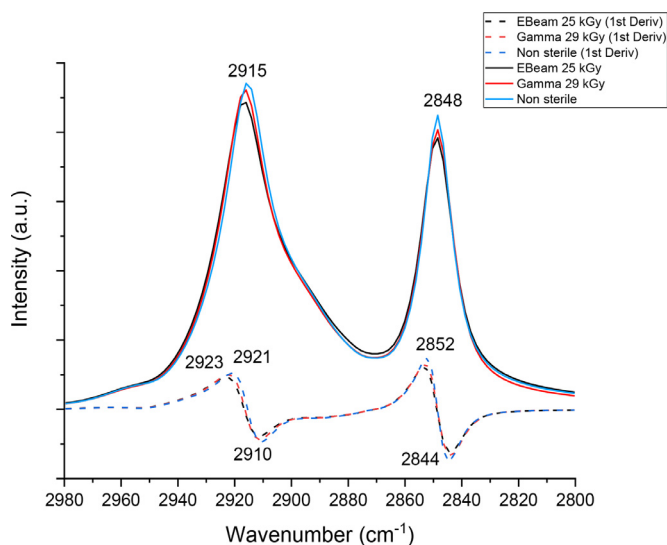


**Fig. 8.** Overlay of derived (after SNV treatment) and pristine sample spectra for electron beam and gamma irradiated samples at ~25 kGy - 6 months after irradiation - spectral zone [3100-2650  $\text{cm}^{-1}$ ].

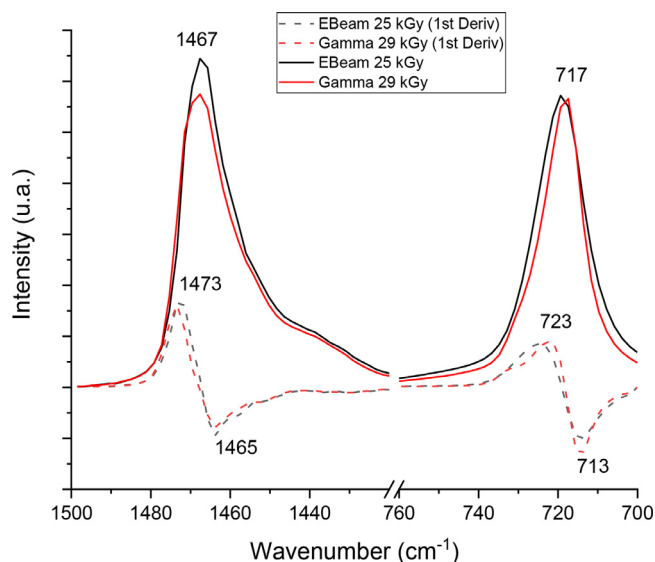


**Fig. 10.** Overlay of derived (after SNV treatment) and natural sample spectra for electron beam and gamma irradiated samples - 1 month after irradiation - zone [1500-1400 & 800-700  $\text{cm}^{-1}$ ].

imately 10% of the spectral variance at A6 (3100-2650  $\text{cm}^{-1}$ ). This difference expresses small variations at the surface level and does not represent variations at the macroscopic level in the material. Crosslinking events discussed in the mechanistic discussion (Section 3.6) do not induce modifications at the macroscopic level and do not affect the thermal properties.

The results observed 24 months after irradiation (6 months at 40 °C) are the same as those observed 6 months after irradiation and the same comments hold. Results are reported in Fig. 6-SI.

After one month ageing, the zones 1500-1400 and 800-700  $\text{cm}^{-1}$ , ascribed to the  $\text{CH}_2$  deformation vibrations in the crystalline and amorphous part, show 2 groups (Fig. 9a). One group formed of electron beam irradiated samples and a group formed of gamma irradiated samples are observed on the plot PC1 vs PC2 (Fig. 9a) accounting for 86% of the total variance. As already reported [21] for gamma irradiation, no difference is observed between non-sterilized samples and the gamma irradiated samples. The gamma irradiated samples and non-sterilized samples present in the positive part of PC1 exhibit high band intensity at 1473 and 717  $\text{cm}^{-1}$  (Fig. 9b). Electron beam irradiated samples present in the negative part of PC1 exhibit high band intensity at 1465, 730 and

723  $\text{cm}^{-1}$  (Fig. 9b). This difference is likely due to the difference in crystallinity in the polymers. The 1465  $\text{cm}^{-1}$  band refers to the amorphous phase whereas the 1473  $\text{cm}^{-1}$  band refers to the crystalline phase [28,29]. It seems that the amorphous phase is greater in the electron beam irradiated samples than the gamma irradiated and non-sterilized samples, because of the rigidification due to the cross-linking. In other words, the electron beam irradiated samples seem to lose a greater part of the crystalline phases than the gamma irradiated samples. Fig. 10 also confirms this observation: the 1467  $\text{cm}^{-1}$  band intensity for the electron beam irradiation (black) is higher than that for gamma irradiation (red). This difference once again expresses small variations at the microscopic level at the surface and does not represent variations at the macroscopic level in the core of the material.

For six month ageing A6, the signal evolution in zones 1500-1400 and 800-700  $\text{cm}^{-1}$  (Fig. 11) is identical to the one observed in the 3100-2650  $\text{cm}^{-1}$  spectral zone (Fig. 7). Upon ageing, gamma and electron beam irradiated samples seem to lose part of their crystalline phase in favour of their amorphous phase. The decrease and shift of the  $-\text{CH}_2$  stretching peak at ~2950  $\text{cm}^{-1}$  linked to the increase in the 1465  $\text{cm}^{-1}$  peak intensity would indicate that elec-

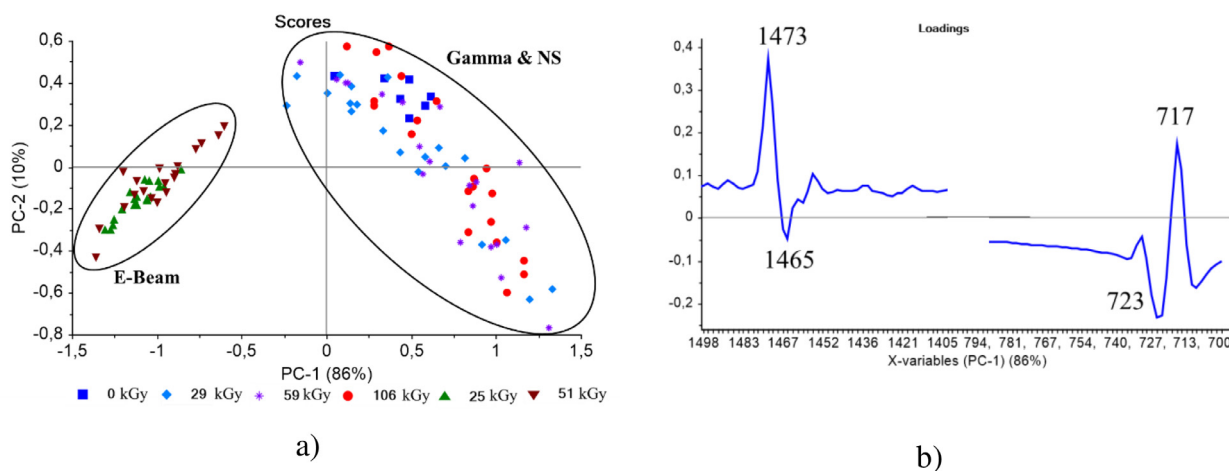
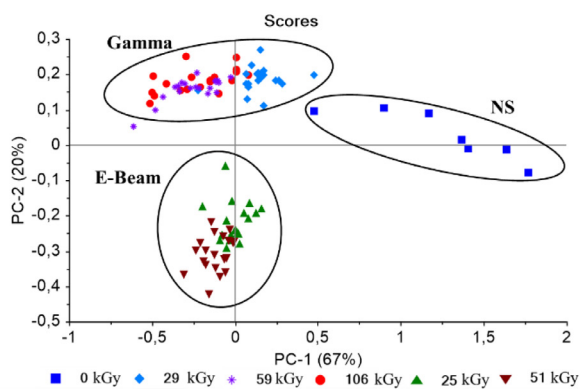
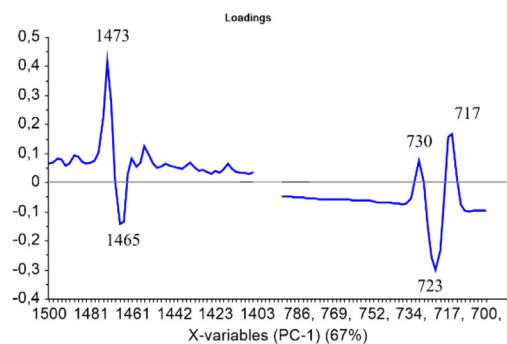


**Fig. 9.** One-month ageing. (a) PCA for all spectra at all absorbed doses for zone (1500-1400 & 800-700  $\text{cm}^{-1}$ ) after baseline and SNV correction. (b) Loading plot of PC1.



a)



b)

**Fig. 11.** Six month ageing. (a) PCA for all spectra at all absorbed doses (1500–1400 & 800–700  $\text{cm}^{-1}$ ) after baseline and SNV correction. (b) Loading plot of PC1.

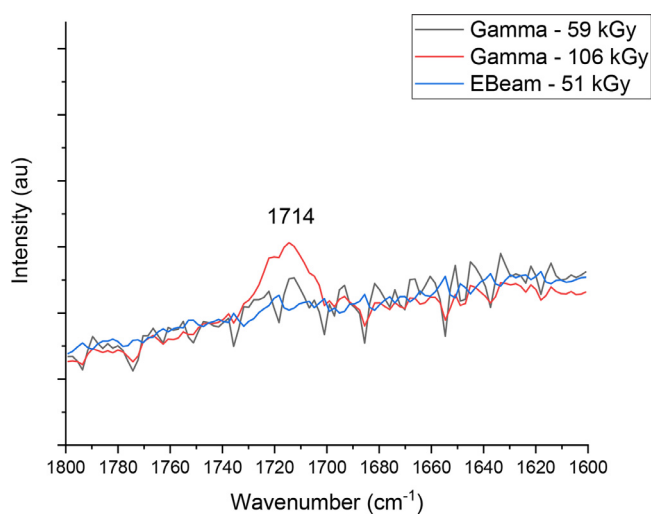


**Fig. 12.** Spectra of gamma irradiated and electron beam irradiated samples >50 kGy.

tron beam irradiation provokes a higher proportion of cross-linking than gamma irradiation does. The same results are observed 24 months (6 months at 40 °C) after irradiation. The behavior of the gamma irradiated samples is close to that of the electron beam irradiated samples, meaning that no more evolution is observed. Results are reported in Fig. 5 in SI.

In the spectral zone 1800–1600  $\text{cm}^{-1}$  at any ageing, the band at 1714  $\text{cm}^{-1}$  (corresponding to the C=O stretching vibration in carboxylic acid) appears only with the sample gamma irradiated

at ~100 kGy (Fig. 12), as already reported [21]. Despite PCA is a powerful tool to enhance weak changes, the small intensity of this band impedes any use of it both for gamma irradiation and electron beam irradiation.

**Mechanism discussion.** As only surface FTIR was performed, the chemistry occurring in the internal EVOH is not discussed. Importantly, we expect same type of reactivity to occur in the PE part of EVOH polymer. Fig. 13 summarize chemical reactions likely to occur during the irradiation of PE. Under irradiation, PE affords an alkyl radical. The latter reacts by coupling with another alkyl radical providing crosslinking events (as proposed in the Sections 3.3 and 3.4.) The alkyl radical can also react with the oxygen present in the atmosphere (as conditions are not controlled) and generate carboxylic acid. The quantity of carboxylic acids directly depends on the irradiation dose [21] and likely the procedure of irradiation. That this the reason why in the Section 3.5, the band corresponding to the C=O stretching vibration in carboxylic acid is weak at doses <100 kGy. The weak signal of carboxy group denotes a weak generation of carboxyl function meaning that the surface is almost protected of influence of  $\text{O}_2$  (see experiment section). The generation of carboxy function occurs likely via a peracid intermediate which decomposes into oxidation products and primary alkyl radical which is either oxidized into carboxy or dimerized for chain lengthening.

The difference in crosslinking products between gamma and electron beam as well as these observed in oxidizing products with reported work are likely due to the kinetics of the reaction. These kinetics depends on the dose received in one shot (electron beam more powerful than gamma) and on the procedure of irradiations which are not controlled (i.e. different companies for electron beam and gamma and for previous work in gamma). Hence, a

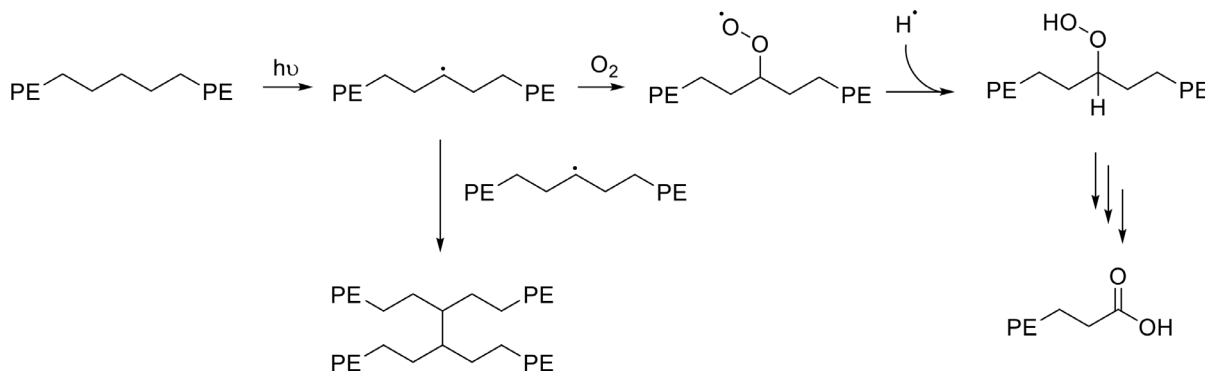


**Fig. 13.** PE reactivity under irradiation.

large amount of alkyl radical generated in a poor O<sub>2</sub> environment will favour crosslinking events over oxidations and fragmentation events and conversely. These crosslinking events are highlighted with FTIR but not with DSC. The recrystallization from molten state is expected and could be lowered if crosslinking occurs even in the amorphous phase [30,31]. All in all, the extent of the crosslinking events is low and will not affect the intended use of the overall material.

#### 4. Conclusion

The modifications occurring in single use plastic bags made up of a PE/EVOH/PE multilayer film up to 24 months (6 months at 40 °C) under gamma and electron beam irradiation in industrial conditions (presence of oxygen not controlled) were assessed. FTIR analyzes were performed on each sample and spectra were evaluated with PCA. Three spectral zones were defined: 3100–2650 cm<sup>-1</sup>, 1500–1400; 800–700 cm<sup>-1</sup> and 1800–1600; 1300–1100 cm<sup>-1</sup>. Different chemical evolutions are observed for gamma and electron beam irradiation. One-month post irradiation, the behavior of the electron beam and gamma irradiated samples is different from that of the non-sterilized sample. Electron beam irradiated samples seem to present a smaller number of CH<sub>2</sub> groups, which is probably due to crosslinking events. Moreover, there seems to be more of the amorphous phases than in the gamma irradiated and non-sterilized samples, which is again probably due to crosslinking events. Six months after irradiation, gamma and electron beam irradiated samples undergo a post irradiation evolution. These different behaviors at 6 and 24 months (6 months at 40 °C) for electron beam and gamma irradiated samples are ascribed to a loss in crystallinity. All in all, the extent of the crosslinking events is low and will not affect the intended use of the overall material. Importantly, no characteristic bands of double bond (3080 cm<sup>-1</sup> (vibration and stretching CH<sub>2</sub> - H of vinyl and vinylidene; 995–980 cm<sup>-1</sup> vinyl group -CH=CH<sub>2</sub>; 895–885 cm<sup>-1</sup> vinylidene C=CH<sub>2</sub>; 980–955 cm<sup>-1</sup> alcene trans; 730–655 cm<sup>-1</sup> alcene cis; 1680–1620 cm<sup>-1</sup> stretching (C = C)) are observed highlighting the absence of chain scission events. The radiation chemistry is the same for gamma and electron beam irradiation however a difference in proportions could be observed. No oxidation band is observed. All the spectroscopic differences observed in this study express small variations at the microscopic level at the surface and does not represent variations at the macroscopic level in the material. Differences are observed by chemometrics which are helpful to amplify small changes. However, when raw data are carefully scrutinized differences are tiny meaning that the impact of irradiation is weak, but it has still an impact on oxidation processes.

#### Declaration of Competing Interest

None.

#### Acknowledgments

N.G.P thanks Sartorius Stedim Biotech for PhD Grant. N.D and S.R.A.M are thankful to AMU and CNRS for their support, and to Sartorius Stedim Biotech for funding. The authors thanks Cécile Grapeloup for her technical support.

#### References

- [1] S. Dorey, S.R.A. Marque, N. Dupuy, M. Murphy, L. Fifield, S.D. Pillai, M. Pharr, D. Staack, L. Nichols, An international industry and academia collaboration to supplement gamma sterilization by X-ray and E-beam technologies, (n.d.).
- [2] P.M. Armenante, O. Akiti, D.J. Ende, M.T. Ende, Sterilization processes in the pharmaceutical industry, Chemical Engineering in the Pharmaceutical Industry: Active Pharmaceutical Ingredients, 1st ed., Wiley, 2019, doi:10.1002/9781119600800.
- [3] S. Moondra, N. Raval, K. Kuche, R. Maheshwari, M. Tekade, R.K. Tekade, Sterilization of pharmaceuticals, Dosage Form Design Parameters (2018) 467–519, doi:10.1016/B978-0-12-814421-3.00014-2.
- [4] D. Darwis, B.Abbas Erizal, F. Nurlidar, D.P. Putra, Radiation processing of polymers for medical and pharmaceutical applications, Macromol. Symp. 353 (2015) 15–23, doi:10.1002/masy.201550302.
- [5] V. Komolprasert, Packaging food for radiation processing, Radiat. Phys. Chem. 129 (2016) 35–38, doi:10.1016/j.radphyschem.2016.07.023.
- [6] J. Mittendorfer, B. Gallnböck-Wagner, Process control in electron beam sterilization of medical devices and a pathway to parametric release, Radiat. Phys. Chem. 173 (2020) 108870, doi:10.1016/j.radphyschem.2020.108870.
- [7] L.S. Fifield, M. Pharr, D. Staack, S.D. Pillai, L. Nichols, J. McCoy, T. Faucette, T.T. Bisel, M. Huang, M.K. Hasan, L. Perkins, S.K. Cooley, M.K. Murphy, Direct comparison of gamma, electron beam and X-ray irradiation effects on single-use blood collection devices with plastic components, Radiat. Phys. Chem. 180 (2021) 109282, doi:10.1016/j.radphyschem.2020.109282.
- [8] W. Kajzer, J. Szewczenko, A. Kajzer, M. Basiaga, J. Jaworska, K. Jelonek, A. Hercog, M. Kaczmarek, A. Marcinkowski, J. Kasperczyk, The effect of electron beam sterilization on the physical properties of the bioresorbable polymer coatings on the titanium 6-aluminum 4-vanadium substrate, Materialwiss. Werkstofftech. 51 (2020) 631–644, doi:10.1002/mawe.201900223.
- [9] O. Mrad, J. Saunier, C. Aymes Chodur, V. Rosilio, F. Agnely, P. Aubert, J. Vigneron, A. Etcheberry, N. Yagoubi, A comparison of plasma and electron beam-sterilization of PU catheters, Radiat. Phys. Chem. 79 (2010) 93–103, doi:10.1016/j.radphyschem.2009.08.038.
- [10] K. Nakamura, Assessment of heat and storage conditions on  $\gamma$ -ray and electron beam irradiated UHMWPE by electron spin resonance, Biomaterials 19 (1998) 2341–2346, doi:10.1016/S0142-9612(98)00150-1.
- [11] T.A.M. Valente, D.M. Silva, P.S. Gomes, M.H. Fernandes, J.D. Santos, V. Sencadas, Effect of sterilization methods on electrospun poly(lactic acid) (PLA) fiber alignment for biomedical applications, ACS Appl. Mater. Interfaces 8 (2016) 3241–3249, doi:10.1021/acsami.5b10869.
- [12] T.J. Madera-Santana, R. Meléndrez, G. González-García, P. Quintana-Owen, S.D. Pillai, Effect of gamma irradiation on physicochemical properties of commercial poly(lactic acid) clamshell for food packaging, Radiat. Phys. Chem. 123 (2016) 6–13, doi:10.1016/j.radphyschem.2016.02.001.
- [13] ISO 11137-1:2006 Stérilisation des produits de santé – Irradiation – partie 1: exigences relatives à la mise au point, à la validation et au contrôle de routine d'un procédé de stérilisation pour les dispositifs médicaux, 2006.
- [14] G. Audran, S. Dorey, N. Dupuy, F. Gaston, S.R.A. Marque, Degradation of  $\gamma$ -irradiated polyethylene-ethylene vinyl alcohol-polyethylene multilayer films: an ESR study, Polym. Degrad. Stab. 122 (2015) 169–179, doi:10.1016/j.polymdegradstab.2015.10.021.
- [15] M. Dole, A commentary on 'free radicals and new end groups resulting from chain scission: 1.  $\gamma$ -irradiation of polyethylene, Polymer 22 (1981) 1458–1459 (Guildf), doi:10.1016/0032-3861(81)90311-6.
- [16] M. Dole, C. Gupta, N. Gvozdić, Crystallinity and crosslinking efficiency in the irradiation of polyethylene, Radiat. Phys. Chem. 14 (1979) 711–720, doi:10.1016/0146-5724(79)90106-7.
- [17] M. Dole, V.M. Patel, comparison of irradiation crosslinking and chain scission in extended chain and bulk film samples of linear polyethylene, Radiat. Phys. Chem. 9 (1977) 433–444, doi:10.1016/0146-5724(77)90159-5.
- [18] M. Driffield, E.L. Bradley, I. Leon, L. Lister, D.R. Speck, L. Castle, E.L.J. Potter, Analytical screening studies on irradiated food packaging, Food Addit. Contam. Part A 31 (2014) 556–565, doi:10.1080/19440049.2013.865087.
- [19] J.C.M. Suarez, E.B. Mano, Characterization of degradation on gamma-irradiated recycled polyethylene blends by scanning electron microscopy, Polym. Degrad. Stab. 72 (2001) 217–221, doi:10.1016/S0141-3910(01)00012-X.
- [20] F. Gaston, N. Dupuy, S.R.A. Marque, M. Barbaroux, S. Dorey, FTIR study of ageing of  $\gamma$ -irradiated biopharmaceutical EVA based film, Polym. Degrad. Stab. 129 (2016) 19–25, doi:10.1016/j.polymdegradstab.2016.03.040.

- [21] F. Gaston, N. Dupuy, S.R.A. Marque, M. Barbaroux, S. Dorey, One year monitoring by FTIR of  $\gamma$ -irradiated multilayer film PE/EVOH/PE, *Radiat. Phys. Chem.* 125 (2016) 115–121, doi:[10.1016/j.radphyschem.2016.03.010](https://doi.org/10.1016/j.radphyschem.2016.03.010).
- [22] The United States Pharmacopeial Convention, USP35 1211 Sterilization and Sterility Assurance, 2012.
- [23] EUROPEAN PHARMACOPEIA 5.0, General texts on sterility, Strasbourg, 2009.
- [24] GIPA, IIA, a comparison of gamma, E-beam, X-ray and ethylene oxide technologies for the industrial sterilization of medical devices and healthcare products, (2017).
- [25] H. Martens, T. Naes, *Multivariate Calibration*, Wiley, New York, 1989.
- [26] F02 Committee, Guide for accelerated aging of sterile barrier systems for medical devices, ASTM International, n.d. doi:[10.1520/F1980-16](https://doi.org/10.1520/F1980-16).
- [27] G. Socrates, *Infrared and Raman characteristic Group frequencies: Tables and Charts*, 3rd.ed., Wiley, Chichester, 2010 repr. as paperback.
- [28] G. Zerbi, G. Gallino, N. Del Fanti, L. Bainsi, Structural depth profiling in polyethylene films by multiple internal reflection infra-red spectroscopy, *Polymer* 30 (1989) 2324–2327 (Guildf), doi:[10.1016/0032-3861\(89\)90269-3](https://doi.org/10.1016/0032-3861(89)90269-3).
- [29] *International Seminar: Thermal Analysis and Rheology*, R. Artiaga Díaz, I. Digitalia, International Seminar, Thermal analysis and rheology, thermal analysis fundamentals and applications to material characterization, in: *Proceedings of the International Seminar–Thermal Analysis and Rheology*, Ferrol, Spain, 2005 30 Juny [sic]–4 July 2003, Universidade da Coruña, Servizo de Publicacións, A Coruña, Spain.
- [30] E. Richaud, P. Ferreira, L. Audouin, X. Colin, J. Verdu, C. Monchy-Leroy, Radiochemical ageing of poly(ether ether ketone), *Eur. Polym. J.* 46 (2010) 731–743, doi:[10.1016/j.eurpolymj.2009.12.026](https://doi.org/10.1016/j.eurpolymj.2009.12.026).
- [31] T. Choupin, Mechanical performances of PEKK thermoplastic composites linked to their processing parameters, Ecole nationale supérieure d'arts et métiers - ENSAM, 2017.